

Supporting Information: Understanding Associative Polymer Self-Assembly with Shrinking Gate Fluorescence Correlation Spectroscopy

Timothy J. Murdoch,[†] Baptiste Quienne,[‡] Julien Pinaud,[‡] Sylvain Caillol[‡] and Ignacio Martín-Fabiani^{†,}*

[†]Department of Materials, Loughborough University, LE11 1RJ Loughborough, United Kingdom

[‡]ICGM, Univ Montpellier, CNRS, ENSCM, Montpellier, France

*corresponding author: Ignacio Martín-Fabiani i.martin-fabiani@lboro.ac.uk

HEUR

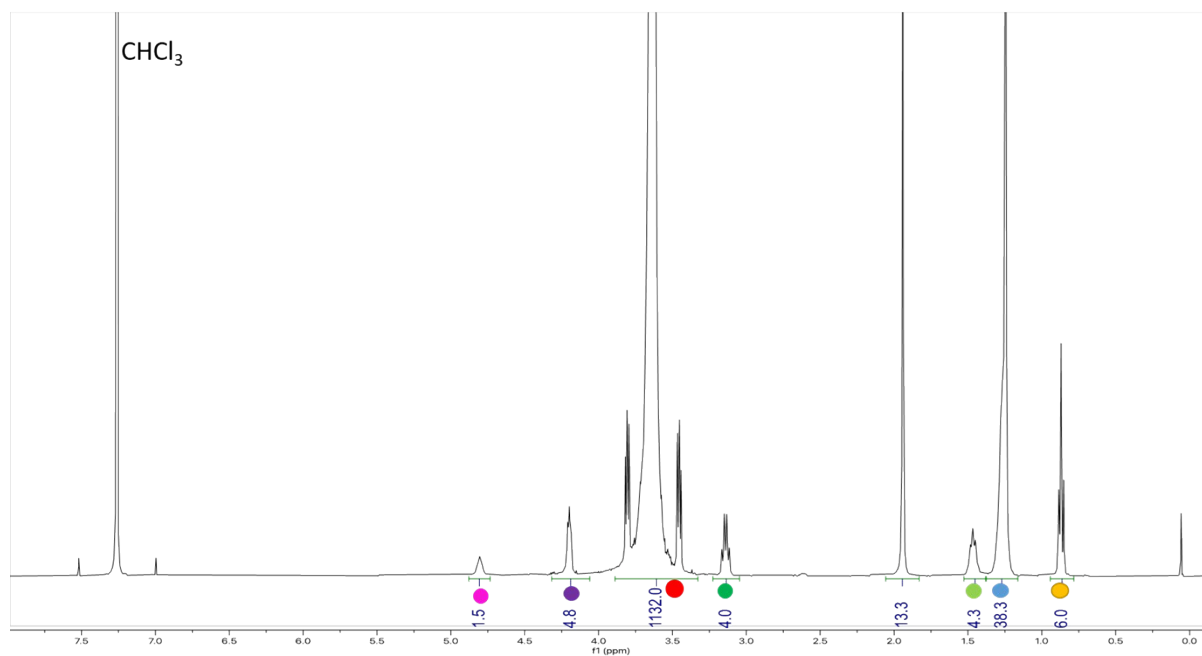
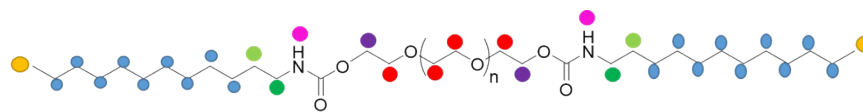


Figure S1. ^1H NMR spectrum of HEUR10kC12

HEUR Rheology

Steady shear rate sweeps were performed using a TA Instruments DHR-2 (New Castle, USA) controlled stress rheometer using a 40 mm diameter stainless steel parallel plate geometry. Temperature was maintained at 25 °C using a Peltier plate. In most cases, a micropipette was used to apply 535 μL of sample directly to the bottom plate. This volume was calibrated at the measurement gap of 0.4 mm by systematically varying the volume of DI water until surface tension artefacts were minimized.¹ No additional pre-shear or flow-conditioning was performed prior to measuring. Data were collected between 0.1 and 1000 s^{-1} with between 3 and 5 logarithmically spaced points per decade. Even with the volume correction, useful data was only measurable above 10 s^{-1} for solutions with viscosity close to water.

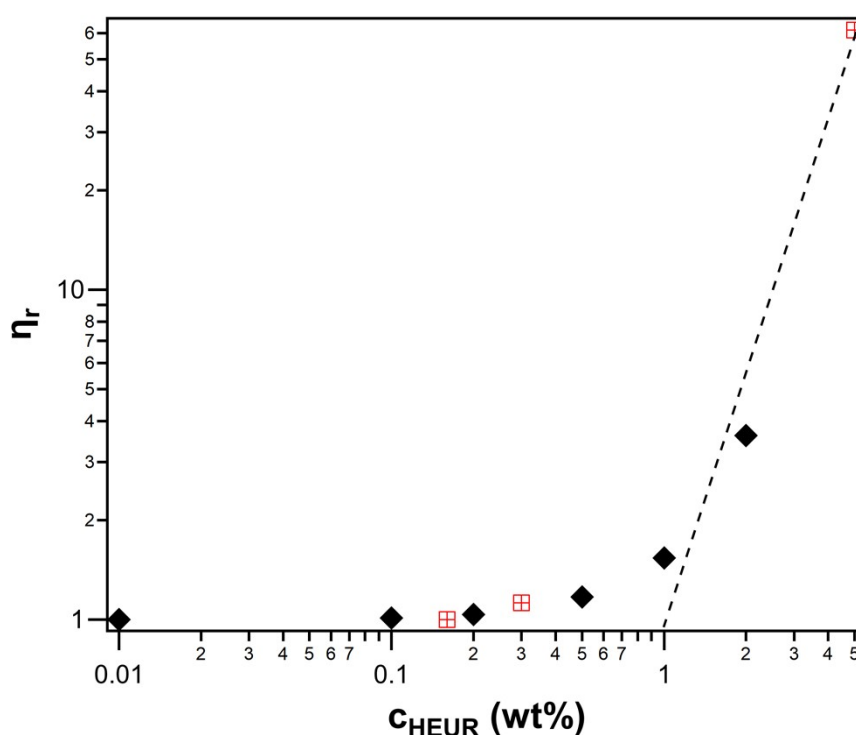


Figure S2. Shear rheology of HEUR10kC12. Filled datapoints are reproduced from Murdoch et al.² while unfilled datapoints correspond to additional measurements for this work. The dotted line is drawn to guide the eye.

Additional Lifetime Figures and Discussion

Influence of Number of Lifetime Components

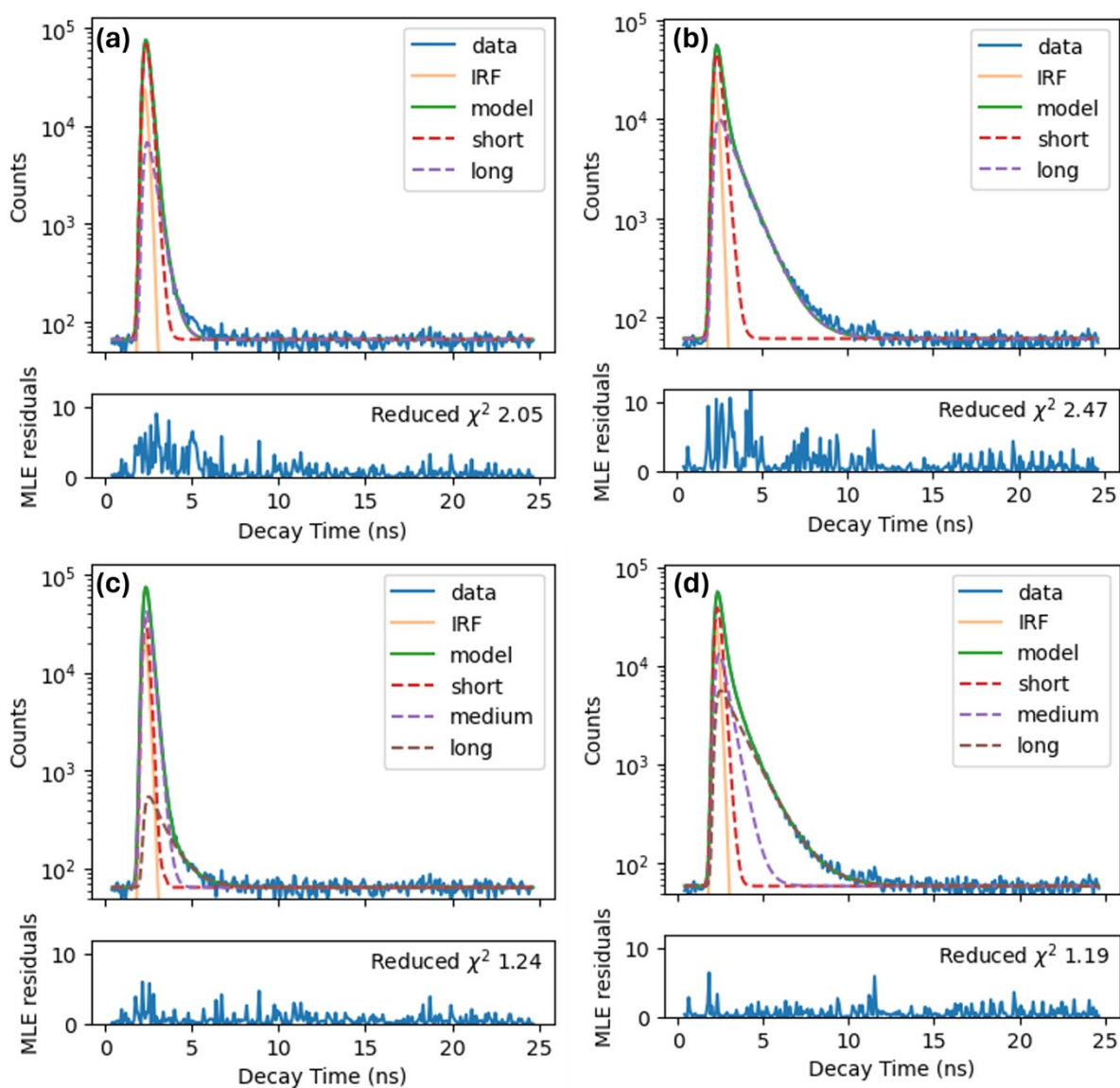


Figure S3. Examples of contributions of individual components to lifetime fitting. (a,c) are at 0.1 wt% HEUR and (b,d) are at 0.1 wt% HEUR. (a,b) use two lifetime components and (c,d) use three lifetime components. At both concentrations the reduced χ^2 is significantly higher using two components. Similarly, the residuals of the maximum likelihood estimator (MLE) for Poisson deviance³ are larger and has greater systematic deviations with two components, compared to three components.

Viscosity Calibration

We calibrate the viscosity-lifetime relationship of sCy3 using a series of glycerol:H₂O mixtures of known viscosity. This leads to a monotonic increase in lifetime with increasing glycerol content (Figure S4a). The lifetime decays were found to be bi-exponential for all conditions except pure H₂O, which was monoexponential (Figure S4b). The shortest exponential component was found to be largely insensitive to change in viscosity.

The Förster Hoffman equation is typically used to describe the relationship between viscosity and the lifetime of molecular rotors. However, it is known that Cy3 does not follow this equation at viscosities greater than 30 cP as the lifetime asymptotically approaches the value corresponding to fully restricted rotation.⁵ Instead, the Hill equation of the intensity average lifetime is found to be more appropriate:⁵

$$\tau = 0.074 + \frac{(1.994 - 0.074)\eta^{0.934}}{\eta^{0.934} + 13.5^{0.934}} \quad (\text{S3})$$

Note that, the intensity average is heavily weighted towards the longest lifetime component, which suggests that this long component is the most sensitive to viscosity changes.

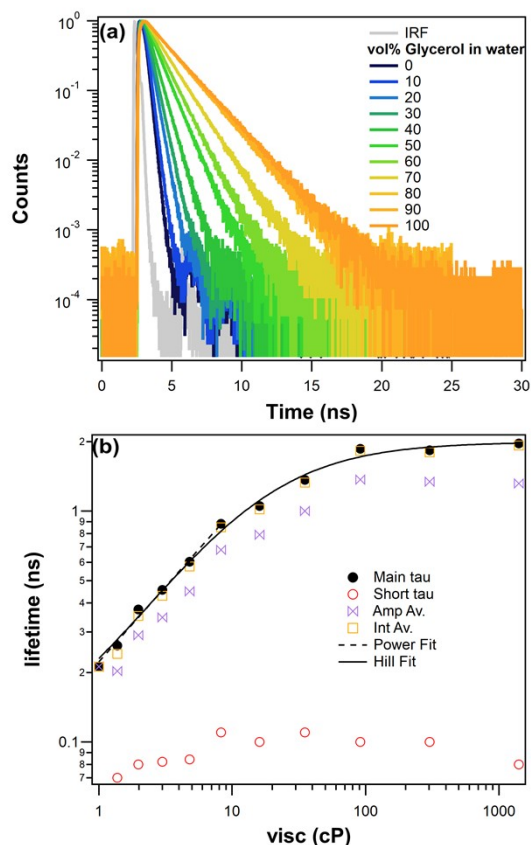


Figure S4. (a) Fluorescence decays in water:glycerol mixtures. (b) Fitted lifetimes vs viscosity. The intensity average lifetime was used for subsequent fitting by a power law and the Hill equation.

Stretched Exponential Fitting

Stretched exponentials have been used in literature to represent distributions of lifetimes.⁴ This can be used to model the intensity, I , as a function of decay time, t :

$$I(t) = IRF * \alpha_{short} e^{-\frac{t}{\tau_{short}}} + IRF * \alpha_{stretch} e^{\left(-\frac{t}{\tau_{stretch}}\right)^\beta} + BKG \quad (S1)$$

where IRF is the instrument response function, α_i and τ_i are the amplitude and characteristic lifetimes, β is the stretching exponent and BKG is the background signal. Subscripts “short” and “stretch” refer to an optional short exponential decay and the stretched exponential contribution, respectively. As seen in Figure S3a, a stretched exponential contribution without the addition of a short exponential decay cannot accurately describe the data. Combining both contributions allows the data to be well-described (Figure S5), with a slightly higher χ^2 value compared to using three exponential components (Figure S3d).

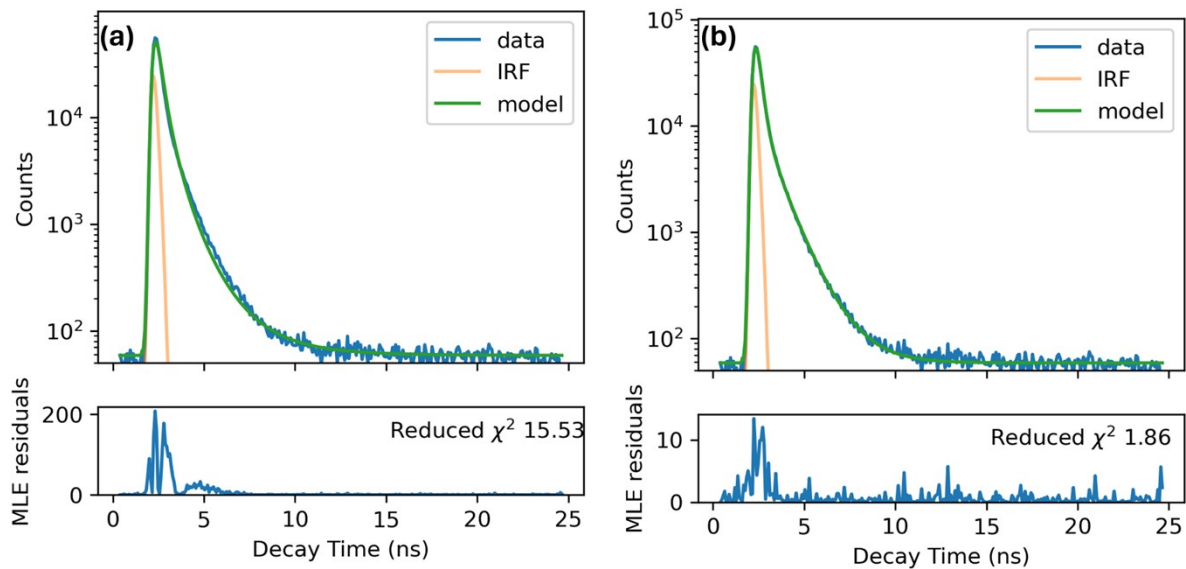


Figure S5 Fitted data and corresponding maximum likelihood estimate (MLE) residuals for (a) a single stretched exponential and (b) a stretched exponential combined with a short exponential decay.

We can calculate the average lifetime of the stretched exponential component by:

$$\tau_{ave,stretch} = \frac{\tau_{stretch}}{\beta} \Gamma\left(\frac{1}{\beta}\right) \quad (S2)$$

where Γ is the gamma function. For the combination of a short exponential and the stretched exponential we have $\beta = 0.73$ and $\tau_{stretch} = 0.44$ ns yielding $\tau_{ave,stretch} = 0.55$ ns. Without the short exponential component, $\tau_{stretch}$ is unstable and hits the lower bound (0.001 ns) and therefore does not provide useful results.

Additional sgFCS Data and Discussion

Fractional Intensity Contribution

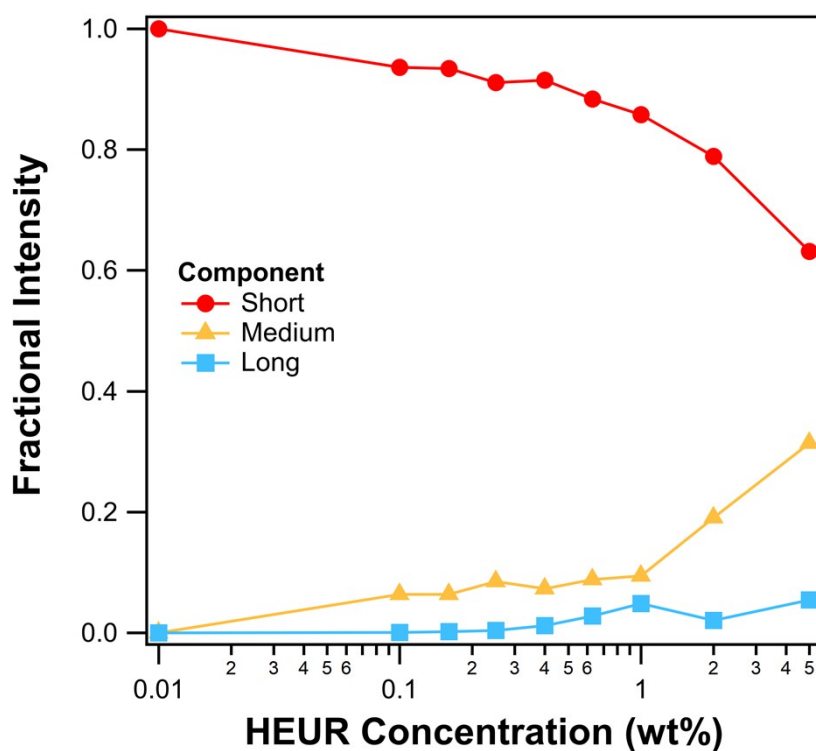


Figure S6. Fractional of total intensity of each lifetime component as a function of HEUR concentration. The analysis assumes that there is no background contribution, and the components are allowed to decay for an infinite period of time.

Reverse Shrinking Gate and Double Diffusion

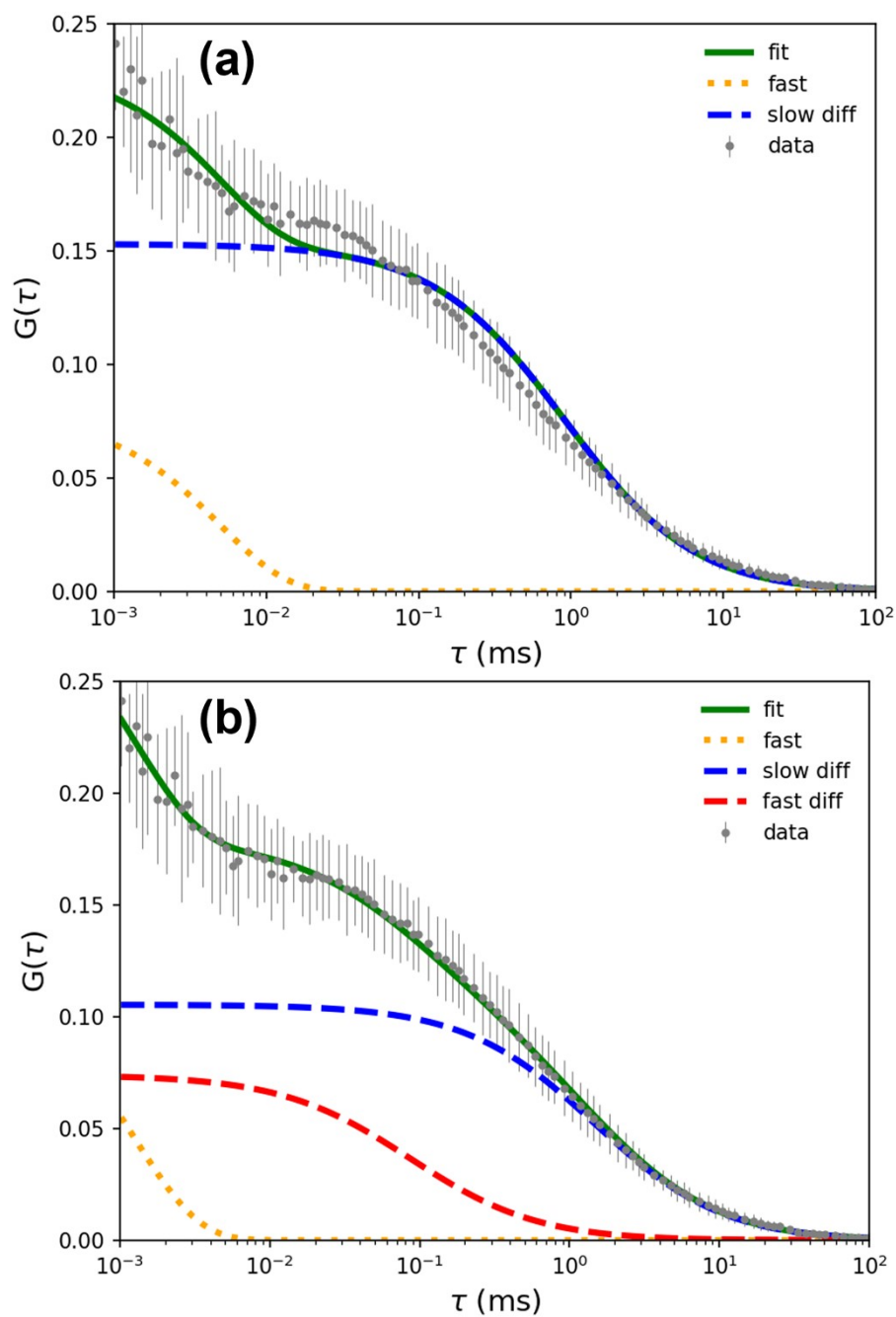


Figure S7. Example fits of 5 wt% HEUR $t_g = 4$ ns with (a) single and (b) double diffusion models.

In the main text, a double diffusion model accounting for free and bound dye was utilized. To reduce the number of free parameters, it was necessary to fix the diffusion time for the free dye, τ_{free} . This was achieved by fitting a single diffusion component to $G(\tau)$ calculated for photons within a short window after the pulse. To confirm the validity of this approach a “reverse” shrinking-gate analysis was performed for a shrinking window of photons from the pulse up to a reverse gate time (t_{rg}) is analyzed (Figure S8a). Analogous to the convergence of $G(\tau)_{norm}$ at high values of t_{rg} , autocorrelation curves at low values of t_{rg} overlap (Figure S8b). This suggests $G(\tau)_{norm}$ at low t_{rg} are dominated by the unbound, short-lifetime dye. A value of 0.55 ns was chosen for t_{rg} , as reduced values of t_{rg} introduced noise associated with low photon counts.

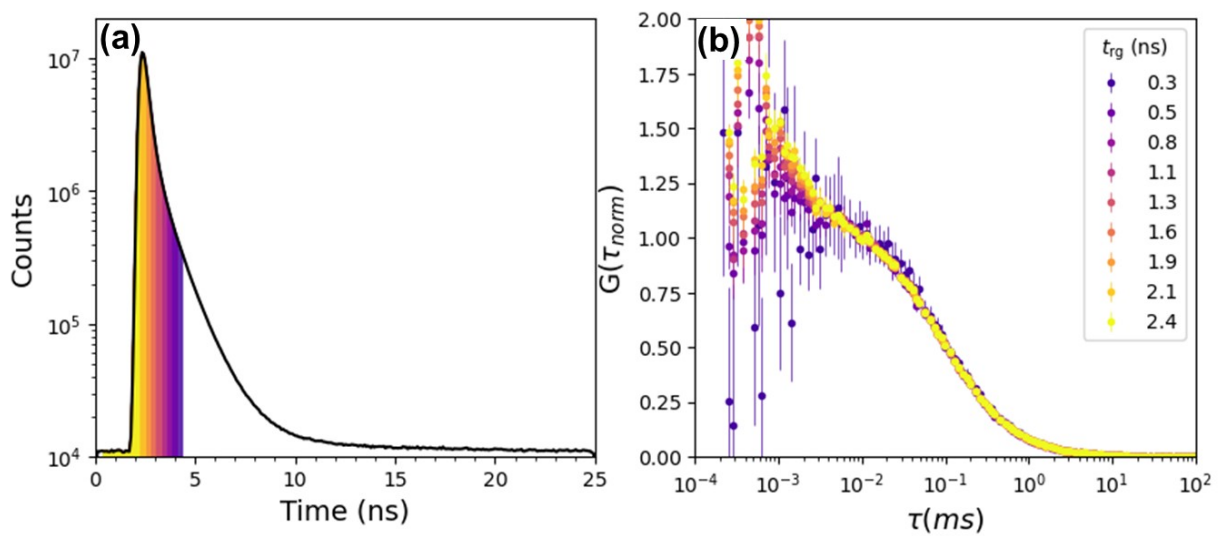


Figure S8. Demonstration of reverse shrinking gate with (a) example fluorescence decay and regions encompassed for each t_{rg} and (b) corresponding normalized autocorrelation curves.

In the vast majority of cases double diffusion fits result in lower reduced χ^2 values. However, these fits have an extra degree of freedom from the fraction of each component. Therefore to inform whether the extra complexity is appropriate we perform an F -test by calculating the ratio of the reduced χ^2 from single and double diffusion fits (Figure S9).⁶ We can compare the resulting F values to critical F values based on the number of datapoints (107), the desired confidence level, and the number of degrees of freedom (5 and 6 for single and double diffusion respectively). This gives critical F values of 1.39 and 1.59 for confidence levels of 95% and 99%, respectively. Note that between 0.25 and 1 wt% HEUR data falls below the critical F values at higher values of t_g where we do not expect free dye. However, double diffusion fits remove systematic deviations in the residuals at time lags corresponding to diffusion and the fact that extracted diffusion coefficients plateau at $t_g > 1.3$ ns gives confidence in the extracted values.

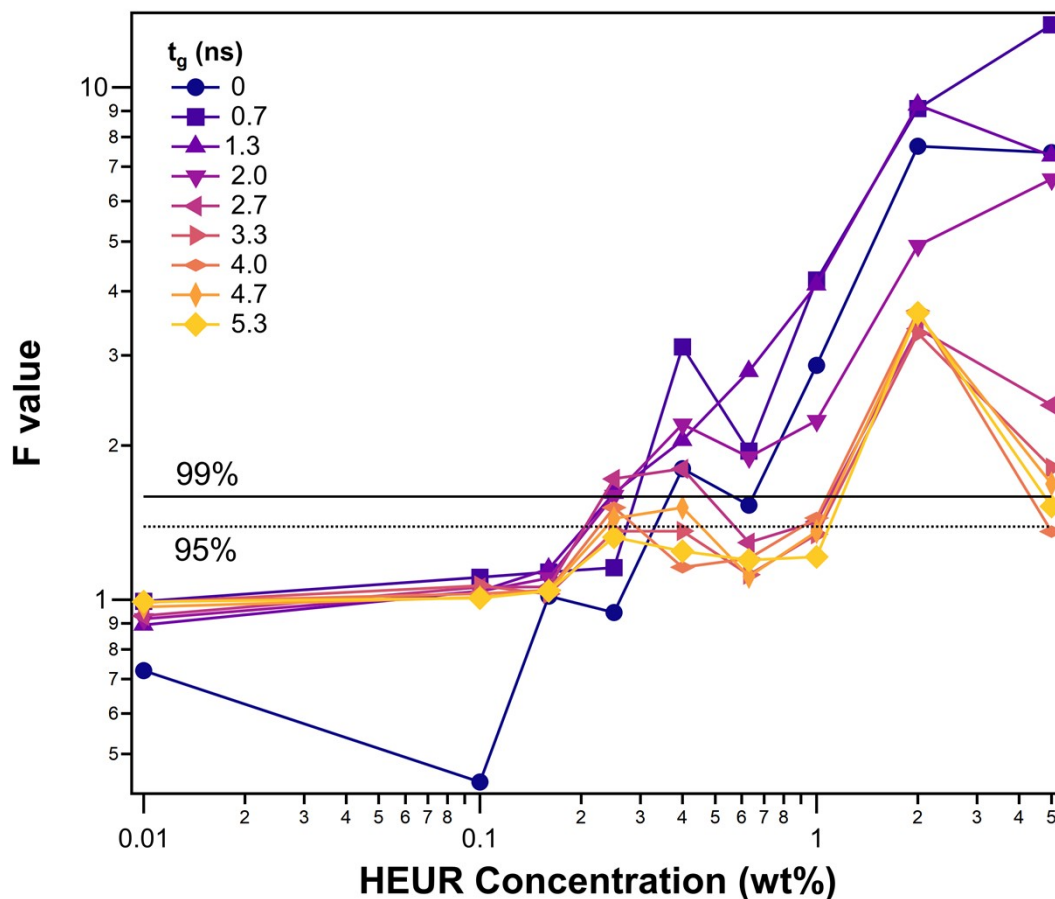


Figure S9. F value comparing Single and Double Diffusion fits. Horizontal lines correspond to the critical F -value at the labelled confidence level.

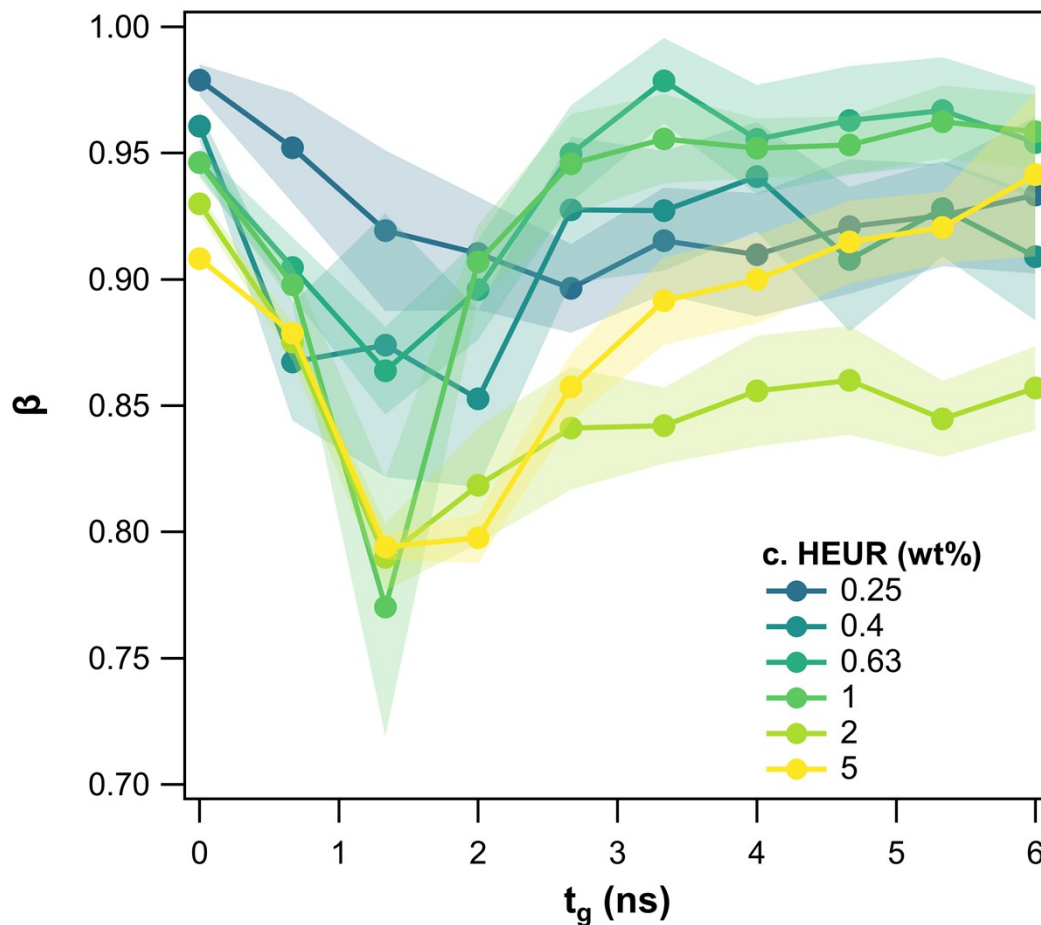


Figure S10. Anomalous diffusion coefficient vs time gate as function of HEUR concentration. Note, the goodness-of-fit for anomalous diffusion is approximately equal to double diffusion fitting. The minima observed between 1 and 2 ns correspond to the presence of free and bound dye, while the values at extreme gate times may correspond obstructed diffusion or the presence of a heterogenous size distribution of aggregates. At concentrations below 0.25 wt% the anomalous diffusion coefficient is within uncertainty of 1.0.

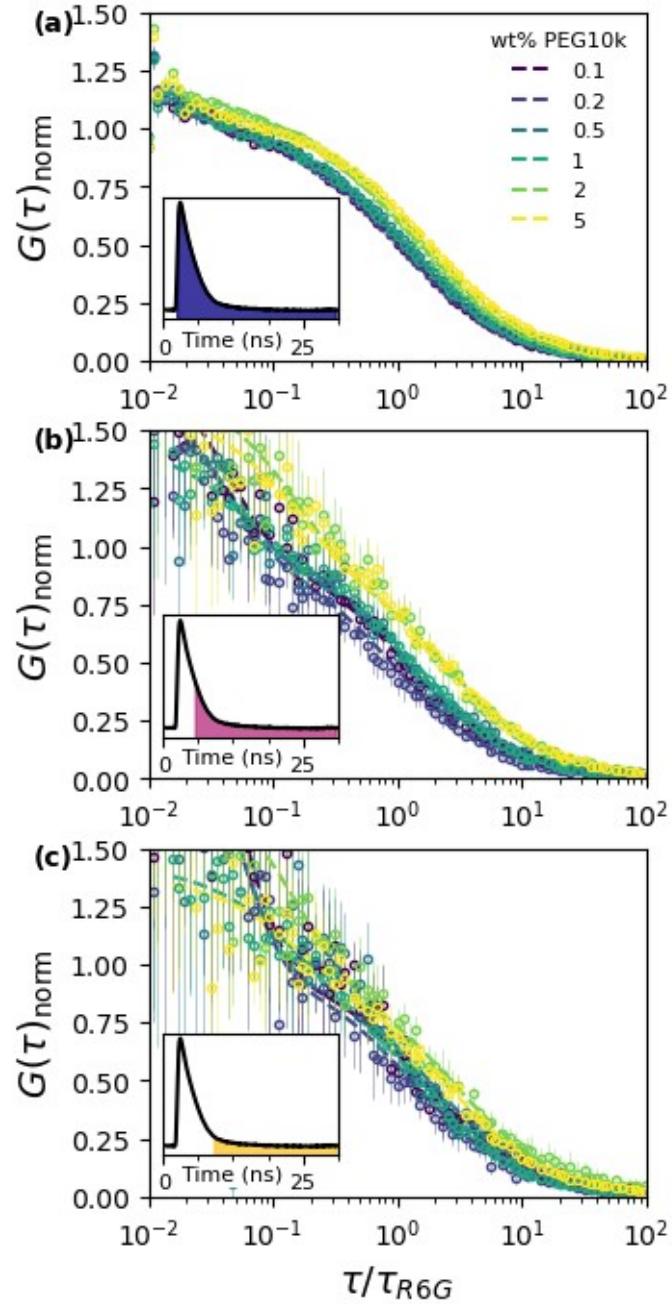


Figure S11. Autocorrelation curves as a function of PEG10k concentration produced by (a) standard FCS and (b) sgFCS with $t_g = 2.7$ ns and (c) $t_g = 5.3$ ns. Note, τ_{R6G} is the characteristic diffusion time of Rhodamine 6G dye used to calibrate the system. Solid and dashed lines correspond to double and single diffusion fits, respectively. *INSET*: Example fluorescence decays where the shaded region indicates the time gate used for analysis.

References

- 1 M. T. Johnston and R. H. Ewoldt, *Journal of Rheology*, 2013, **57**, 1515–1532.
- 2 T. J. Murdoch, B. Quienne, M. Argaiž, R. Tomovska, E. Espinosa, F. D'Agosto, M. Lansalot, J. Pinaud, S. Caillol and I. Martín-Fabiani, *ACS Appl. Polym. Mater.*, 2023, **5**, 6672–6684.
- 3 Ž. Bajzer, T. M. Therneau, J. C. Sharp and F. G. Prendergast, *European Biophysics Journal*, 1991, **20**, 247–262.
- 4 K. C. Benny Lee, J. Siegel, S. E. D. Webb, S. Lévêque-Fort, M. J. Cole, R. Jones, K. Dowling, M. J. Lever and P. M. W. French, *Biophysical Journal*, 2001, **81**, 1265–1274.
- 5 N. A. Hosny, C. Fitzgerald, A. V. Vyšniauskas, A. Athanasiadis, T. Berkemeier, N. Uygur, M. Shiraiwa, M. Kalberer, F. D. Pope, M. K. Kuimova, U. Pöschl, M. Shiraiwa, M. Kalberer, F. D. Pope and M. K. Kuimova, *Chemical Science*, 2016, **7**, 1357–1367.
- 6 U. Meseth, T. Wohland, R. Rigler and H. Vogel, *Biophysical Journal*, 1999, **76**, 1619–1631.